

---

# Implicit Variational Conditional Sampling with Normalizing Flows

---

**Vincent Moens**  
Huawei R&D UK  
vincentmoens@gmail.com

**Aivar Sootla**  
Huawei R&D UK

**Haitham Bou Ammar**  
Huawei R&D UK  
University College London

**Jun Wang**  
Huawei R&D UK  
University College London

## Abstract

We present a method for conditional sampling with normalizing flows when only part of an observation is available. We rely on the following fact: if the flow’s domain can be partitioned in such a way that the flow restrictions to subdomains keep the bijectivity property, a lower bound to the conditioning variable log-probability can be derived. Simulation from the variational conditional flow then amends to solving an equality constraint. Our contribution is three-fold: a) we provide detailed insights on the choice of variational distributions; b) we propose how to partition the input space of the flow to preserve bijectivity property; c) we propose a set of methods to optimise the variational distribution in specific cases. Through extensive experiments, we show that our sampling method can be applied with success to invertible residual networks for inference and classification.

## 1 Introduction

Conditional data generation is a ubiquitous and challenging problem, even more so when the data is high dimensional. In some settings, the partitioning of the conditioned data and conditioning itself can be established in advance. In those cases a wide variety of tools can be used to achieve the inference task depending on the problem formulation, ranging from Bayesian inference [14] and its approximations (e.g. variational inference [28]) to Gaussian [6] or Neural Processes [13]. Normalizing flows (NFs) [43] have recently emerged as a new tool to achieve this kind of conditional inference in the Maximum-Likelihood setting.

The task is considerably more interesting yet harder when this partitioning cannot be anticipated. Its uses span a wide range of applications, from few shots learning [52] to super resolution image generation [2], high-dimensional Bayesian optimisation [37, 15], learning with incomplete datasets [54, 33, 44], image inpainting [12] and many more.

When the assumption can be made that the data is distributed according to a Gaussian distribution, the conditional distribution can be derived in closed form, an observation that paves the way for Gaussian Processes (GPs) solutions [6] and alike. Although they constitute a solid component of the modern machine learning toolbox, these solutions are not well suited for a variety of problems. The Gaussian assumption is, in fact, quite restrictive in nature: GPs are in their vanilla form used for problems where the observations are uni-dimensional and where inference has to be performed on a subset of these variables. As a consequence, alternative tools may need to be used when dealing with even moderately high dimensional data, or equivalently when part of the input data can be missing.

It is well-established that NFs can model arbitrarily complex joint distributions. Furthermore, they naturally embed together the joint probability of any partition of data that could occur during training or at test time. Hence, it is tempting to make use of NFs to solve such tasks. Nonetheless, only a few works have successfully investigated how this model family can be used for this scope.

This work pursues this goal in the following settings, either in isolation or in combination: first, conditional data generation may need to be performed once a model has been trained, regardless of the fact that the existence of incomplete data was known before training. Second, training data may be itself incomplete, in the sense that some training features might be missing from examples in the training dataset. Third, the subset of data that is missing may not be known in advance, and it could also be randomly distributed across input data.

Importantly, we are interested in deriving a method whereby the distribution of the data generated faithfully reflects the one that could be expected from a Bayesian perspective.

The paper is organised as follows. In Section 2, we give account of the state of the art and shortly introduce how our solution fits in the existing literature. Given this perspective, in Section 3, we present our method, and give a detailed account of the theoretical and practical implications that follow from our problem formulation. Section 4 displays the experimental results obtained over a diversity of NFs architectures and tasks.

## 2 Prior work and Contribution

A few existing works have studied the problem of conditional data generation with NFs. A first line of work, provided by [7], used Projected Latent Monte Carlo chains to generate samples that converge in probability to the desired conditional distribution. The advantage of this method is that the distribution of samples that are gathered using this technique will converge to the true conditional probability distribution as the chain gets longer. However, one can identify several drawbacks that are to be considered: first, as for every other Monte Carlo sampling method, the mixing time cannot be known in advance, and hence one may wonder whether the samples that are gathered truly belong to the conditional distribution. In practice, long chains may be required to obtain convincing results. Second, albeit the observed part of the imputed data converges towards the true observed values, a difference between the two may persist. Third, training a model comprising missing data with PL-MCMC is achieved through a Monte Carlo Expectation Maximisation (MCEM) scheme [10, 39]. Under appropriate assumptions, MCEM is guaranteed to converge to a local maximiser of the the log-likelihood function, but this is conditioned on the quality of the data generated by the Monte Carlo algorithm. Consequently, as the optimisation progresses towards the optimum, longer chains may be required to ensure convergence [39].

MCFlow [44] constitutes another landmark in the domain of conditional data generation with NFs. This method relies on an auxiliary feedforward neural network whose role is to produce latent embeddings with maximum a posteriori likelihood values. Those values are constrained to lie on the manifold of latent vectors whose mapping to the observed space match the observations. MCFlow produces state-of-the-art results in terms of image quality or classification accuracy when compared to GAN-based methods such as [54, 33]. However, this method is tailored to fit NFs when the training data is incomplete, and requires a set of adjustment to the model. As such, it cannot be applied to post-training data completion as PL-MCMC.

It is also worth mentioning that several conditioning techniques have been used with NFs in contexts where the joint probability distribution of the conditioning and conditioned random variable is of no interest. For instance, [43, 4] extended to the parameters of the flow the amortization technique used in Variational Auto-Encoders (VAEs) to infer the parameters of the variational posterior [25]. [53] extended this use to the scenario of conditional likelihood estimation, while [50] provided a Variational Bayes view on this problem by using a Bayesian Neural Network as a conditioning feature embedder. On a different line of work, [27] use a heuristic form of *a posteriori* conditioning. The generative flow is trained with a classifier over the latent space, which forces the latent representation location to be indicative of the class they belong to. At test time, some parametric distribution is fitted on the latent representations to account for the attributes of the images that are to be generated. [40] used a hybrid approach, whereby the conditioning and conditioned variables joint distribution is modelled by a normalizing flow in such a way that conditional sampling of one given the other is

straightforward to apply. Still, either with this approach or the others above, the knowledge of what part of the data constitutes the conditioning random variable is still required beforehand.

**Our contribution** We provide a method to efficiently infer missing data at train and test time when using normalizing flows, in the setting where one has not access in advance to the observed/hidden partitioning of the data. The usage of a variational posterior brings numerous advantages: for example, with a single fitted posterior, multiple samples can quickly be recovered. We also show that we can amortize the cost of inference across multiple partially observed items through the use of inference networks [25].

### 3 Method

#### 3.1 Variational conditional distribution with normalizing flows

Let us consider a generic  $C^1$ -diffeomorphism  $f(\mathbf{X}) : \mathcal{X} \rightarrow \mathcal{Y}$  where  $\mathcal{X} \subseteq \mathbb{R}^d$ ,  $\mathcal{Y} \subseteq \mathbb{R}^d$ , which admits an inverse  $g(\mathbf{y}) \equiv f^{-1}$ . We denote their respective Jacobians as  $\mathbf{J}(\mathbf{x}) = \nabla_{\mathbf{x}} f(\mathbf{x})$  and  $\mathbf{G}(\mathbf{y}) = \nabla_{\mathbf{y}} g(\mathbf{y})$ . We denote by  $\mathbf{J}$  the detached version of  $\mathbf{J}(\mathbf{x})$ , i.e. a matrix whose values match those of  $\mathbf{J}$  but have a null gradient. Consider the case where  $f \# P_0$  encodes a distribution over the random variable  $\mathbf{Y} = f(\mathbf{X})$  when  $\mathbf{X}$  is distributed according to the base distribution  $P_0(\mathbf{X})$  with density  $p_0(\mathbf{x})$ . In what follows, we assume that  $P_0$  can be factorised as a product of independent univariate distributions. Using the change of variable rule, it follows that  $\mathbf{Y}$  has a log-density given by the following formula:

$$\begin{aligned} \log p(\mathbf{y}) &= \log p_0(g(\mathbf{y})) + \log |\det \nabla_{\mathbf{y}} g(\mathbf{y})| \\ &= \log p_0(\mathbf{x}) - \log |\det \nabla_{\mathbf{x}} f(\mathbf{x})|. \end{aligned} \quad (1)$$

Our goal is to sample from the conditional distribution over a partial observation  $\mathbf{Y}^O \in \mathcal{Y}^O$  where  $\mathcal{Y}^O = \{\mathbf{y}^O \mid \mathbf{y} \in \mathcal{Y}\}$  and  $\mathcal{Y}^H = \{\mathbf{y}^H \mid \mathbf{y} \in \mathcal{Y}\}$  for some index  $O_{\mathcal{Y}} \subset [d]$  with cardinality  $\#O_{\mathcal{Y}} = d^O$ ,  $d^O < d$  and its complement  $H_{\mathcal{Y}} \subset [d]$ ,  $\#H_{\mathcal{Y}} = d^H$ . This distribution has a density given by  $p(\mathbf{y}^H \mid \mathbf{y}^O) = \frac{p(\mathbf{y})}{p(\mathbf{y}^O)}$ , where  $p(\mathbf{y}^O) = \int p(\mathbf{y}^O, \mathbf{y}^H) d\mathbf{y}^H$  is in general intractable.

Throughout this paper, we make the following assumption on the flow  $f$  and its inverse  $g$ :

**Assumption 1** *There exists a partition  $\mathcal{X}^O = \mathcal{X} \setminus \mathcal{X}^H$  with indexes  $O_{\mathcal{X}} = [d] \setminus H_{\mathcal{X}}$  such that the restriction of  $f$ ,  $f^O(\mathbf{X}^O; \mathbf{X}^H) : \mathcal{X}^O \rightarrow \mathcal{Y}^O$  is a  $C^1$ -diffeomorphism for all  $\mathbf{x}^H \in \mathcal{X}^H$ . Additionally, we assume that the eigenvalues of the inverse Jacobian of  $f^O$  are bounded.*

Crucially, the partitioning of  $\mathcal{X}$  is somewhat arbitrary, and does not need to match the one of  $\mathcal{Y}$  (i.e.  $O_{\mathcal{Y}}$  does not necessarily match  $O_{\mathcal{X}}$ ). Assumption 1 may appear quite restrictive in practice, and hence deserves a thorough discussion. We empirically found that for a the class of NFs where the blocks are encoded as residual layers, this assumption is mild and a suitable partition can be found with little effort. Some architectures (e.g. Glow [27] or RealNVPs [11]) may not enjoy this property. Consequently, the results presented here are exclusively obtained while using the invertible residual network (iResNet) family of models [3, 9]. We give more details on the choice of the partitioning of the latent space in Section 3.6.

The following lemma follows immediately from Assumption 1:

**Lemma 1** *If there exists a restriction of a diffeomorphism  $f$ ,  $f^O(\mathbf{X}^O; \mathbf{X}^H) : \mathcal{X}^O \rightarrow \mathcal{Y}^O$ , as defined in Assumption 1, then there must exist a complementary restriction of  $g = f^{-1}$ , namely  $g^H(\mathbf{y}^H; \mathbf{y}^O) : \mathcal{Y}^H \rightarrow \mathcal{X}^H$ , that is also a diffeomorphism for all  $\mathbf{y}^O \in \mathcal{Y}^O$ .*

The proof of Lemma 1 follows directly from the Schur decomposition of the Jacobian matrix of  $f$ , and is given in Appendix A.

Based on this observation, we reformulate the log-absolute value (LAD) of the Jacobian determinant to reformulate Eq 1 as

$$\log p(\mathbf{y}) = \log p_0(\mathbf{x}^H) + \log |\det \nabla_{\mathbf{y}^H} g^H(\mathbf{y}^H; \mathbf{y}^O)| + \log p_0(\mathbf{x}^O) - \log |\det \nabla_{\mathbf{x}^O} f^O(\mathbf{x}^O; \mathbf{x}^H)|. \quad (2)$$

This reformulation is central to our work: our plan is to utilise the fact that the joint log probability of the observed and generated data can be equivalently split in the base distribution space. Although

they do not equate each other in general (i.e.  $\log p(\mathbf{y}) \neq \log p_0(\mathbf{x}^O) - \log |\det \nabla_{\mathbf{x}^O} f^O(\mathbf{x}^O; \mathbf{x}^H)|$ ), we can employ this structure to generate  $\mathbf{y}^H$  given a distribution over  $\mathbf{x}^H$  that is to be defined.

We consider the variational lower bound to  $\log p(\mathbf{y}^O)$  given by the variational distribution  $q(\mathbf{y}^H; \mathbf{y}^O) = q(\overline{\mathbf{x}^H}) \left| \det \nabla_{\mathbf{y}^H} \overline{\mathbf{x}^H} \right|$  (where, with a slight abuse of notation, we have used  $\overline{\mathbf{x}^H} \equiv g^H(\mathbf{y}^H; \mathbf{y}^O)$  as a reparameterised sample) that it to approximate  $p(\mathbf{y}^H | \mathbf{y}^O)$ :

$$\begin{aligned} \mathcal{L}(q(\mathbf{y}^H; \mathbf{y}^O)) &= \mathbb{E}_{q(\mathbf{y}^H; \mathbf{y}^O)} [\log p(\mathbf{y}^H, \mathbf{y}^O)] + \mathbb{H} [q(\mathbf{y}^H; \mathbf{y}^O)] \\ &= \mathbb{E}_{q(\mathbf{y}^H; \mathbf{y}^O)} \left[ \log \frac{p_0(\overline{\mathbf{x}^H})}{q(\overline{\mathbf{x}^H})} + \log p_0(\overline{\mathbf{x}^O}(\overline{\mathbf{x}^H}, \mathbf{y}^O)) - \log \left| \det \nabla_{\overline{\mathbf{x}^O}} f^O(\overline{\mathbf{x}^O}(\overline{\mathbf{x}^H}, \mathbf{y}^O); \overline{\mathbf{x}^H}) \right| \right] \\ &= \mathbb{E}_{q(\mathbf{x}^H)} \left[ \log \frac{p_0(\mathbf{x}^H)}{q(\mathbf{x}^H)} + \log p_0(\overline{\mathbf{x}^O}(\mathbf{x}^H, \mathbf{y}^O)) - \log \left| \det \nabla_{\overline{\mathbf{x}^O}} f^O(\overline{\mathbf{x}^O}(\mathbf{x}^H, \mathbf{y}^O); \mathbf{x}^H) \right| \right] \end{aligned} \quad (3)$$

where  $\mathbb{H}[\cdot]$  is the entropy of the distributions it takes as argument,

$$\overline{\mathbf{x}^O}(\mathbf{x}^H, \mathbf{y}^O) = \mathbf{x}^O \Big|_{f^O(\mathbf{x}^O; \mathbf{x}^H) - \mathbf{y}^O = 0}$$

is a reparameterised variable belonging to  $\mathcal{X}^O$  and where we have taken advantage of the fact that the LAD of the Jacobian belonging to the approximate posterior  $q(\mathbf{y}^H; \mathbf{y}^O)$  cancels with the one from the joint log-probability given by the model.

The existence of this bound suggests a two-pass iterative algorithm aimed at sampling from a conditional normalizing flow using a parametric posterior  $q_\theta(\mathbf{y}^H | \mathbf{y}^O)$  (Algorithm 1): first, given the current configuration of the approximate posterior  $q_\theta(\mathbf{y}^H | \mathbf{y}^O)$ , a set of conditional samples is drawn by solving the equality given by  $F_{\mathbf{y} \rightarrow \mathbf{x}}(\mathbf{y}^H; \mathbf{y}^O, \mathbf{x}^H) = g^H(\mathbf{y}^H; \mathbf{y}^O) - \mathbf{x}^H = 0$  or, equivalently, by  $F_{\mathbf{x} \rightarrow \mathbf{y}}(\mathbf{x}^O; \mathbf{x}^H, \mathbf{y}^O) = f^O(\mathbf{x}^O; \mathbf{x}^H) - \mathbf{y}^O = 0$ . By design, the latter will usually be easier to solve than the former as the observed topological space  $\mathcal{Y}$  will be harder to navigate than the latent one,  $\mathcal{X}$ . Next, this sample is reparameterised given the variational posterior parameters, and lastly an optimisation step is made given the stochastic estimate of the ELBO gradient.

---

**Algorithm 1:** Variational conditional sampling with normalizing flows

---

- 1 **Input:** Base distribution  $p_0(\mathbf{x})$ , invertible flow  $f = g^{-1} : \mathcal{X} \rightarrow \mathcal{Y}$ , partial (masked) observation  $\mathbf{y}^O = m^O(\mathbf{y})$
  - 2 **Output:** Conditional sample  $\mathbf{y}^H \sim p(\cdot | \mathbf{y}^O)$
- initialization: set  $q_\theta(\mathbf{x}^H)$ , select partitioning function  $\mathbf{x}^O - m^O(\mathbf{x})$  // Sections 3.5, 3.6
- while** has not converged **do**
- sample  $\mathbf{x}^H \sim q_\theta(\mathbf{x}^H)$ ;
  - solve for  $\mathbf{x}^O$   $F_{\mathbf{y} \rightarrow \mathbf{x}}(\mathbf{y}^H; \mathbf{y}^O, \mathbf{x}^H) = f^O(\mathbf{x}^O; \mathbf{x}^H) - \mathbf{y}^O = 0$  // Section 3.2
  - reparameterise  $\mathbf{x}^O(\mathbf{x}^H, \mathbf{y}^O, \theta)$  // Section 3.3
  - compute stochastic gradient estimate  $\nabla_\theta \mathcal{L}(q)$  and update variational posterior // Section 3.4
- end**
- 

As a side note, the bound in Eq 3 gets to zero whenever  $\overline{\mathbf{x}^O}$  is independent of  $\mathbf{x}^H$  and when  $q_\theta(\mathbf{x}^H) = p_0(\mathbf{x}^H)$  almost everywhere. In all other cases, this bound can be reduced by optimising the value of  $\theta$  such that the value of  $\mathcal{L}(q_\theta)$  is maximised. The remainder of this section is dedicated to detailing how this can be achieved.

### 3.2 Solving the equality constraint

Let us assume that the partitioning of  $\mathcal{X}$  is known. We face the problem of solving the equation

$$F_{\mathbf{y} \rightarrow \mathbf{x}}(\mathbf{y}^H; \mathbf{y}^O, \mathbf{x}^H) = f^O(\mathbf{x}^O; \mathbf{x}^H) - \mathbf{y}^O = 0. \quad (4)$$

We consider two root-finding approaches: a new fixed-point iterative algorithm and Newton-Krylov methods. In practice, we used the latter as a fallback option when the former did not converge below the desired convergence threshold.

**Fixed-point iterative algorithm** As our method heavily relies on solving equality constraints, one may wish to reduce the computational burden of this operation. We therefore seek for an efficient gradient-free method that can achieve this in some settings. To this aim, we consider the following iterative approach, whose convergence properties is analysed in Theorem 1, whose proof is given in Appendix B:

---

**Algorithm 2:** Variational conditional sampling with normalizing flows

---

- 1 **Input:** Invertible flow  $f = g^{-1}$ , partial (masked) observation  $\mathbf{y}^O = m^O(\mathbf{y})$ , conditional latent hidden sub-vector  $\mathbf{x}^H$ , mixing coefficients  $\{\alpha, \beta\} \in (0, 1]$
  - 2 **Output:** Solutions  $(\mathbf{y}^H, \mathbf{x}^O) = f(\mathbf{x}^O, \mathbf{x}^H) - [\mathbf{y}^O; \mathbf{y}^H]^\top = 0$   
 initialization:  $\chi^O = 0$ ;  
 $\mathbf{y}^H = f^H(\chi^O, \mathbf{x}^H)$ ;  
 $\widetilde{\mathbf{x}}^O = \mathbf{x}^O = g^O(\mathbf{y}^O, \mathbf{y}^H)$ ;  
**while** has not converged **do**  
      $\mathbf{y}^H = f^H(\widetilde{\mathbf{x}}^O, \mathbf{x}^H)$ ;  
      $\widetilde{\mathbf{y}}^H = \alpha \mathbf{y}^H + (1 - \alpha) \widetilde{\mathbf{y}}^H$ ;  
      $\mathbf{x}^O = g^O(\mathbf{y}^O, \widetilde{\mathbf{y}}^H)$ ;  
      $\widetilde{\mathbf{x}}^O = \beta \mathbf{x}^O + (1 - \beta) \widetilde{\mathbf{x}}^O$ ;  
**end**
- 

**Theorem 1** Consider Algorithm 2, assume that there exists a unique solution  $\widetilde{\mathbf{x}}^O = g^O(\mathbf{y}^O, \widetilde{\mathbf{y}}^H)$ ,  $\widetilde{\mathbf{y}}^H = f^H(\widetilde{\mathbf{x}}^O, \mathbf{x}^H)$  around which  $g^O$  and  $f^H$  are continuously-differentiable, and the global Lipschitz constants of  $f^H$  and  $g^O$  are equal to  $L_a$  and  $L_b$ , respectively. Then the algorithm converges to the unique solution for any  $\alpha \in (0, 1]$ ,  $\beta \in (0, 1]$ , if  $L_a L_b < 1$ .

We empirically found that in most cases and across several architectures (iResNet, Planar, Radial, Sylvester and Implicit flows), accurately partitioning the latent space such that the volume of the Jacobian  $\mathbf{J}^{OO} = \nabla_{\mathbf{x}^O} f^O(\mathbf{x}^O, \mathbf{x}^H)$  was maximised incidentally lead to well behaving optimisation schedules.

**Newton-Krylov methods:** If the conditions stated in Theorem 1 are not met, an alternative solver needs to be used. If and when Algorithm 2 did not converge, we relied on Newton-Krylov methods [29] instead. Using first order expansion of the flow restriction, we can update  $\mathbf{x}_t^O$  using the iterative procedure  $\mathbf{x}_{t+1}^O = \mathbf{x}_t^O - s \left( \nabla_{\mathbf{x}_t^O} F_{\mathbf{x} \rightarrow \mathbf{y}}(\mathbf{x}^O; \mathbf{x}^H, \mathbf{y}^O) \right)^{-1} F_{\mathbf{x} \rightarrow \mathbf{y}}(\mathbf{x}^O; \mathbf{x}^H, \mathbf{y}^O)$  for a given step size  $s$ . The reliance of this method on the inverse Jacobian-vector product  $\mathbf{J}^{OO^{-1}} \mathbf{u}$  with  $\mathbf{J}^{OO} = \nabla_{\mathbf{x}_t^O} F_{\mathbf{x} \rightarrow \mathbf{y}}(\mathbf{x}^O; \mathbf{x}^H, \mathbf{y}^O)$  requires us to invert a sub-matrix (defined by the input and output masks) that, in most cases, is only accessible via left or right vector-matrix product, due to the constraints imposed by the use of backward propagation algorithms. Moreover, explicit computation of this sub-Jacobian is also usually prohibitively expensive to retrieve in closed form. Therefore, to compute this product involving an inverse sub-Jacobian, we rely on the generalized minimal residual method (GMRES) [45], a Krylov subspace method [46]. At their core, Newton-Krylov methods [29] rely on the computational amortisation of the GMRES-based inversion step by caching intermediate values between successive iterations of the solver [1], which accelerates the clock-time convergence of the algorithm. Still, computing a single Jacobian vector product can still be quite computationally expensive in some instances, for instance when using invertible residual networks [9, 3] (see below). Hence, one may wish to further reduce the cost of this inversion, either via reformulation of the problem or preconditioning. Both approaches rely on the Schur complement identity:

$$\mathbf{J}^{OO^{-1}} = \mathbf{G}^{OO} - \mathbf{G}^{OH} \mathbf{G}^{HH^{-1}} \mathbf{G}^{HO} \quad (5)$$

where  $\mathbf{G} = \mathbf{J}^{-1}$ . Eq 5 gives an alternative formulation of  $\mathbf{J}^{OO^{-1}}$ . This inverse requires us to invert a sub-Jacobian (namely  $\mathbf{G}^{HH^{-1}}$ ), presumably using GMRES or a similar technique. In that case, the inverse of the sub-Jacobian can be obtained or approximated only by querying Jacobian-vector products involving  $\mathbf{G}$ , and not  $\mathbf{J}$ , which can sometimes be more involving. Amongst other notable

possible advantages, inverting  $\mathbf{G}^{HH}$  may be faster to compute if  $d^O > d^H$ , or if  $\mathbf{G}^{HH}$  is easier to precondition.

Otherwise, when computing the plain inverse of  $\mathbf{J}^{OO}$  using GMRES, we used  $\mathbf{G}^{OO}$  as a preconditioner. We found this to speed up the computation by a factor of 2 to 4, depending on the size of the problem and the architecture used.

### 3.3 Reparameterising solutions

We use the implicit function theorem to reparameterise  $\mathbf{x}^O$  as a function of  $\mathbf{x}^H$ ,  $\mathbf{y}^O$  and  $\boldsymbol{\theta}$  if needed:

$$\nabla_{\mathbf{x}^H} \overline{\mathbf{x}^O} = -(\nabla_{\mathbf{x}^O} F_{\mathbf{x} \rightarrow \mathbf{y}}(\mathbf{x}^O; \mathbf{x}^H, \mathbf{y}^O))^{-1} \nabla_{\mathbf{x}^H} F_{\mathbf{x} \rightarrow \mathbf{y}}(\mathbf{x}^O; \mathbf{x}^H, \mathbf{y}^O).$$

As for the Newton-Krylov method (3.2) and for the approximate posterior optimisation (3.5), the product of the inverse of the sub-Jacobian can be obtained via GMRES with similar considerations regarding methods to speed up this computation. Reparameterising as a function of the variational posterior parameters  $\boldsymbol{\theta}$  is then trivially achieved via pathwise or implicit gradient calculation.

### 3.4 Stochastic gradient of the ELBO

Deriving the gradient of the ELBO (Eq 3) requires us to estimate the gradient of the LAD of the sub-Jacobian  $\log |\det \mathbf{J}^{OO}(\mathbf{x}^H)|$  with respect to the reparameterised sample  $\mathbf{x}^H$ . To achieve this, we rely on the observation that the gradient of the LAD can be expressed as

$$\nabla_{\mathbf{x}} \log |\det \mathbf{J}(\mathbf{x})| = \nabla_{\mathbf{x}} \text{Tr} [\mathbf{J}^{-1} \mathbf{J}(\mathbf{x})]$$

where we have made the dependence of  $\mathbf{J}$  on  $\mathbf{x}$  explicit where needed. Hence, although the value of  $\log |\det \mathbf{J}^{OO}(\mathbf{x})|$  cannot be estimated in closed form, its gradient only requires us to differentiate the trace of the product of  $\mathbf{J}^{OO^{-1}}$  and  $\mathbf{J}^{OO}(\mathbf{x})$ , where only the latter is to be differentiated through. As noted before,  $\mathbf{J}$  may only be implicitly defined by its inverse  $\mathbf{G}$  (e.g.  $\mathbf{J}$  is obtained through Neumann series or Krylov methods). In such cases, higher order derivatives cannot be accessed readily by backpropagating through the graph. We present two alternative forms for this gradient: first, using the same identity as in Eq 2, we can reformulate the log absolute Jacobian as

$$\log |\det \mathbf{J}^{OO}(\mathbf{x})| = \log |\det \mathbf{J}(\mathbf{x})| + \log |\det \mathbf{G}^{HH}(f(\mathbf{x}))|, \quad (6)$$

and differentiate this expression directly (assuming that higher order derivatives can be obtained for  $\mathbf{G}$ ). Second, and relying on the masking function  $m^{OO}(\mathbf{J}) = \mathbf{J}^{OO}$  which we use for clarity, we can express the differential equation

$$\nabla_{\mathbf{x}} \text{Tr} [m^{OO}(\mathbf{J})^{-1} m^{OO}(\mathbf{J}(\mathbf{x}))] = \nabla_{\mathbf{y}} \text{Tr} [m^{OO}(\mathbf{J})^{-1} m^{OO}(\mathbf{G}^{-1} \mathbf{G}(\mathbf{y}) \mathbf{G}^{-1})] \nabla_{\mathbf{x}} \mathbf{y}. \quad (7)$$

which follows the fact that  $\partial \mathbf{X}^{-1} = -\mathbf{X}^{-1} \partial \mathbf{X} \mathbf{X}^{-1}$  [42]. We refer to the estimator in Eq 6 as the corrected LAD gradient estimator (CLADE) and to the one in Eq 7 as the natural LAD gradient estimator (NLADE). As before, this formula makes it possible to compute the gradient of the trace operator when higher order derivatives can be obtained from  $\mathbf{G}$  but not (or at a greater cost) from  $\mathbf{J}$ . Both expressions have their advantages and possible drawbacks: if the LAD of  $\mathbf{J}$  can be accessed without approximation and/or if  $d^H \ll d^O$ , the CLADE variance will usually be lower when a stochastic trace estimator is used. If either of these conditions does not hold, the contrary may verify.

### 3.5 On the form of the variational posterior

We used two distinct designs of approximate posterior depending on the task at hand. When possible, each data to be completed was treated separately, with a single variational posterior configuration being fitted to each item in the dataset. When the amount of incomplete items was too large to be completed on a one-to-one basis, we used amortized the cost of inference by acquiring the variational posterior parameters through a inference network that was trained to minimize the KL divergence in Equation 3. More details can be found in Appendix C.

### 3.6 Building bijective restrictions

The choice of the the partition of the latent space  $\mathcal{X}$  in  $\mathcal{X}^O$  and  $\mathcal{X}^H$  is central to our approach and deserves a closer look. With iResNet [3, 9], the structure of the flow naturally leads to a partitioning

of the latent space where the indices match those of the observed space, i.e.  $O_{\mathcal{X}} = O_{\mathcal{Y}}$ . This observation also holds for flows that share a similar residual structure  $f(\mathbf{x}) = \mathbf{x} + h(\mathbf{x})$ , such as Planar and Radial flows [43], Sylvester flows [4], continuous flows [8, 41, 36] or – to some extent – Implicit NFs [35], where at each layer  $t$  of the flow, the derivative of the output  $x_{t+1}^i$  with respect to the input layer  $x_t$  will be dominated by the  $i^{\text{th}}$  component of this input.

## 4 Experiments

### 4.1 Experimental setup

We tested our variational conditional sampling algorithm on a classification and data completion task when the training and test data were partially observed, and on a post-training data completion task. Due to the restriction imposed by Assumption 1, we only considered the iResNet [3, 9] architecture to test our approach on in the main text. Appendix D provides results with Implicit NFs, showing that our approach can be extended to other types of architectures with possibly higher Lipschitz constants. Several steps of our gradient computation rely on computing the inverse of the Jacobian of the transform. This quantity was queried using Neumann series: at each layer  $i \in [L]$  of a  $L$ -deep network, we locally computed the product of a vector with the inverse Jacobian as

$$\mathbf{u}\mathbf{J}_i^{-1} = \mathbf{u} \sum_{j=0}^{\infty} -(\nabla_{\mathbf{x}}h(\mathbf{x}))^j.$$

In practice, the sum was truncated when the difference between two successive iterations was below a predefined small threshold  $\epsilon$ . Jacobian-vector products were computed using the identity  $\mathbf{J}(\mathbf{x})\mathbf{u} = \mathbf{u}\nabla_{\mathbf{v}}[\mathbf{v}\mathbf{J}(\mathbf{x})]$  for some  $\mathbf{v}$ . As this formula requires a graph to be built on top of another one, and to avoid memory overflow, we computed this quantity locally at each layer of the network.

At early stages of training, Algorithm 2 quickly converged with  $\alpha = \beta = 1$ . However, lower values were needed later on, or when using a fully trained model (in the post-training data imputation setting). Therefore, we adopted the following schedule throughout the training process: an initial mixing rate was set to  $\alpha = \beta = 0.5$ , and at each iteration of Algorithm 2, the mixing rate was decayed by a factor of 0.95. Infrequently (less than 1% of the iterations), our fixed-point algorithm did not reach the convergence threshold. In those cases, a Newton-Krylov solver was used. Overall, was moderately computationally expensive: in the case of MNIST dataset, each optimisation step took approximately 20 seconds, roughly equally split between solving the equality constraint retrieving the gradient estimate.

### 4.2 Experimental results

#### 4.2.1 Quantitative experiment: Training on incomplete MNIST data

To test the capability of Implicit Variational Conditional Normalizing Flows (IVCNFs) to learn from incomplete data, we used the MNIST dataset [32] where a percentage of the pixels of each digit image was missing. We only considered the setting where the missing pixels were randomly spread across the image. The NF component consisted in a iResNet model with 73 convolutional layers with 128 channels each, followed by four fully connected residual layers. The remaining network specifics were similar to [9]. The inference network consisted in a 5-layer convolutional network with a  $3 \times 3$  kernel, SAME-padding strategy and with [4, 8, 16, 32, 8] channels at each layer, respectively. For this network, the ReLU activation function [38] was used. Finally, we used a simple classifier consisting of the sequence of a squeezing layer, a 1-dimensional batch-norm layer [21] and a bias-free linear layer. We used the Adam optimiser [26] with a learning rate of  $10^{-2}$ , decaying by a factor of 0.5 at every epoch. The batch size was set to 64 digits, and the components were trained simultaneously for a total of 5 epochs. The NLADE gradient estimator was used for these experiments with the Hutchinson stochastic trace estimator [20], taking a single sample for each gradient computation. We compared our results to the ones presented in PL-MCMC [7], MCFLOW [44] and MisGAN [33]. Due to the limits of our computational resources, we resort on the performances displayed in [44, 7]. All the presented results are computed on MNIST official test dataset, which was not used for training. Figure 1 gives a visual account of the performance of the IVCNF data completion capability. In all cases, IVCNF was either first or second ranked in terms of Top-1 classification accuracy

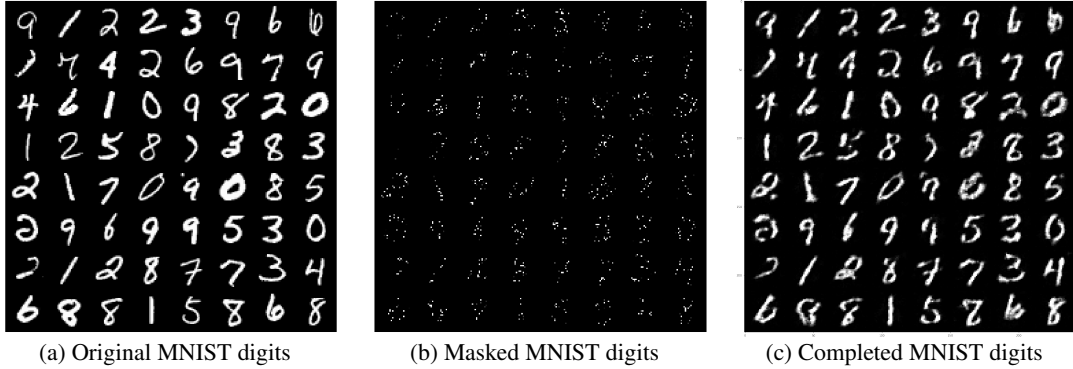


Figure 1: MNIST completion with 90% missingness rate.

(Table 1), Fréchet Inception Score (FID [18], Table 2) or Root-Mean-Squared-Error (RMSE, Table 3). It is important to note that, although MCFLOW outperformed our approach on some occasions, this algorithm relies on the assumption that one can train a separate classifier on complete data, and then use this classifier on the completed dataset. Our IVCNF classifier was, instead, trained on-the-fly on the incomplete dataset only.

Table 1: Top-1 classification accuracy on incomplete MNIST dataset (higher is better)

Missing rate →	0.5	0.6	0.7	0.8	0.9
MisGAN	0.968	0.945	0.872	0.690	0.334
PL-MCMC	-	-	-	-	-
MCFLOW	<b>0.985</b>	<b>0.979</b>	<b>0.963</b>	0.905	0.705
IVCNF (ours)	0.9616	0.9588	0.9485	<b>0.9355</b>	<b>0.886</b>

Table 2: FID on incomplete MNIST dataset (lower is better)

Missing rate →	0.5	0.6	0.7	0.8	0.9
MisGAN	0.3634	0.8870	1.324	2.334	<b>6.325</b>
PL-MCMC	-	5.7	-	-	87
MCFLOW	0.8366	0.9082	1.951	6.765	15.11
IVCNF (ours)	<b>0.2692</b>	<b>0.4398</b>	<b>0.7823</b>	<b>1.5491</b>	7.315

Table 3: RMSE on incomplete MNIST dataset (lower is better)

Missing rate →	0.5	0.6	0.7	0.8	0.9
MisGAN	0.12174	0.13393	0.15445	0.19455	0.27806
PL-MCMC	-	0.1585	-	-	0.261
MCFLOW	<b>0.10045</b>	<b>0.11255</b>	<b>0.12996</b>	0.15806	0.20801
IVCNF (ours)	0.1127	0.1221	0.1340	<b>0.1470</b>	<b>0.1924</b>

#### 4.2.2 Qualitative experiment: post-training data imputation

We now turn to the problem of completing an partially observed item using the IVCNF technique. We trained a standard iResNet-164 architecture on the CIFAR-10 dataset [31] for 250 epochs. IVCNF completion capability was compared to PL-MCMC, as MCFLOW requires the model to be tailored for data completion. The task was similar to the one presented in [7]: a masked centered square of size  $8 \times 8$  had to be completed. PL-MCMC completion was achieved using the same hyperparameters provided by the authors. For IVCNF, we used a Gaussian approximate posterior with a sparse approximation to the covariance matrix encoded by 50 Householder layers. The parameters were trained using the Adam optimiser with a learning rate of  $10^{-2}$ , and at each step, a batch of 8 completed images were generated to obtain a gradient estimate. A total of 500 steps showed to be sufficient to reach convergence. Figure 2a shows how our algorithm compared with PL-MCMC for a set of test images. We also included the first solution obtained by the initial standard Gaussian distribution to show that, although training did make the images look more convincing, the initial guess was already somewhat well fitted to the rest of the image. As a qualitative measure of fitness, we measured the RMSE between generated and true images for both algorithms, and obtained a similar value for both

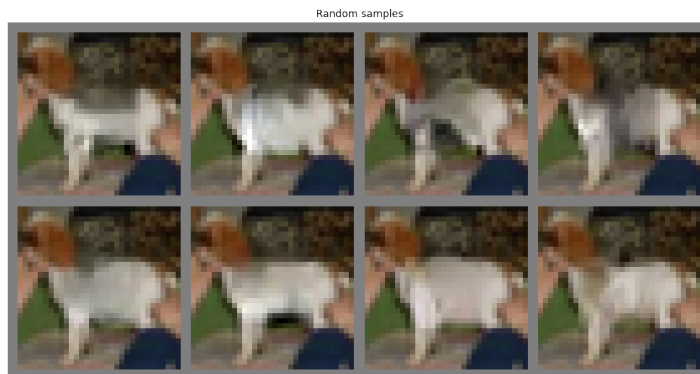


(IVCNF (NLADE):  $0.2291 \pm 0.1570$ , PL-MCMC:  $0.2287 \pm 0.1961$ ). By comparison, at the first iteration of the IVCNF algorithm, an RMSE of  $0.2802 \pm 0.1188$  was measured.

As the gradient of the variational posterior parameters can be retrieved with two different methods (CLADE or NLADE), we compared one against the other, but observed little qualitative or quantitative difference between the two (RMSE for IVCNF (CLADE):  $0.2320 \pm 0.1793$ ).



(a) IVCNF and PL-MCMC post-training data completion



(b) Random samples obtained from an IVCNF-trained variational posterior

A noticeable advantage of IVCNF is that with a single fit of the variational posterior can generate a wide variety of candidate images with little effort, as only a few seconds are needed to solve the equality constraint depicted above. Figure 2b gives some flavour of this capability.

## 5 Limitation and future works

This article presents IVCNF, a new method for data completion with NFs. This technique can be successfully applied to architectures when the units of the flow are made of instances residual layers. For some important classes of NFs (e.g. composed of coupling flows, such as Glow [27] or RealNVP [11]), we did not find methods to efficiently partition of the latent space or solve the equality constraint entailed by our algorithm. Future work should focus on finding alternative ways to fit low-dimensional variational posteriors for data completion in those cases.

## References

- [1] A. H. Baker, E. R. Jessup, and T. Manteuffel. “A Technique for Accelerating the Convergence of Restarted GMRES”. In: *SIAM Journal on Matrix Analysis and Applications* 26.4 (Jan. 2005), pp. 962–984. DOI: 10.1137/s0895479803422014. URL: <https://doi.org/10.1137/s0895479803422014>.
- [2] Syed Muhammad Arsalan Bashir, Yi Wang, and Mahrukh Khan. *A Comprehensive Review of Deep Learning-based Single Image Super-resolution*. 2021. arXiv: 2102.09351 [cs.CV].
- [3] Jens Behrmann et al. *Invertible Residual Networks*. 2019. arXiv: 1811.00995 [cs.LG].
- [4] Rianne van den Berg et al. “Sylvester normalizing flows for variational inference”. In: *proceedings of the Conference on Uncertainty in Artificial Intelligence (UAI)*. 2018.
- [5] David M. Blei, Alp Kucukelbir, and Jon D. McAuliffe. “Variational Inference: A Review for Statisticians”. In: *Journal of the American Statistical Association* 112.518 (2017), pp. 859–877. ISSN: 1537274X. DOI: 10.1080/01621459.2017.1285773. arXiv: 1601.00670.
- [6] C. E. Rasmussen & C. K. I. Williams. *Gaussian processes for machine learning*. Vol. 14. 2. 2006, pp. 1–219. ISBN: 026218253X. DOI: 10.1142/S0129065704001899. URL: <http://www.gaussianprocess.org/gpml/chapters/>.
- [7] Chris Cannella, Mohammadreza Soltani, and Vahid Tarokh. “Projected Latent Markov Chain Monte Carlo: Conditional Sampling of Normalizing Flows”. In: *International Conference on Learning Representations*. 2021. URL: <https://openreview.net/forum?id=MBpHUFrcG2x>.
- [8] Ricky T. Q. Chen et al. “Neural Ordinary Differential Equations”. In: (2018), pp. 1–12. ISSN: 0140-525X. DOI: arXiv:1806.07366v3. arXiv: 1806.07366. URL: <http://arxiv.org/abs/1806.07366>.
- [9] Ricky T. Q. Chen et al. *Residual Flows for Invertible Generative Modeling*. 2020. arXiv: 1906.02735 [stat.ML].
- [10] A. P. Dempster, N. M. Laird, and D. B. Rubin. “Maximum Likelihood from Incomplete Data Via the EM Algorithm”. In: *Journal of the Royal Statistical Society: Series B (Methodological)* 39.1 (1977), pp. 1–22. DOI: <https://doi.org/10.1111/j.2517-6161.1977.tb01600.x>. eprint: <https://rss.onlinelibrary.wiley.com/doi/pdf/10.1111/j.2517-6161.1977.tb01600.x>. URL: <https://rss.onlinelibrary.wiley.com/doi/abs/10.1111/j.2517-6161.1977.tb01600.x>.
- [11] Laurent Dinh, Jascha Sohl-Dickstein, and Samy Bengio. *Density estimation using Real NVP*. 2017. arXiv: 1605.08803 [cs.LG].
- [12] Omar Elharrouss et al. “Image Inpainting: A Review”. In: *Neural Processing Letters* 51.2 (Dec. 2019), pp. 2007–2028. DOI: 10.1007/s11063-019-10163-0. URL: <https://doi.org/10.1007/s11063-019-10163-0>.
- [13] Marta Garnelo et al. *Conditional Neural Processes*. 2018. arXiv: 1807.01613 [cs.LG].
- [14] Andrew Gelman. *Bayesian Data Analysis, Third Edition*. 3rd. Chapman and Hall/CRC, Nov. 2013. ISBN: 9781439898208. DOI: 10.1201/b16018. URL: <https://www.taylorfrancis.com/books/9781439898208>.
- [15] Rafael Gómez-Bombarelli et al. “Automatic Chemical Design Using a Data-Driven Continuous Representation of Molecules”. In: *ACS Central Science* 4.2 (2018). PMID: 29532027, pp. 268–276. DOI: 10.1021/acscentsci.7b00572.
- [16] Louis Guttman. “Enlargement Methods for Computing the Inverse Matrix”. In: *The Annals of Mathematical Statistics* 17.3 (1946), pp. 336–343. DOI: 10.1214/aoms/1177730946. URL: <https://doi.org/10.1214/aoms/1177730946>.

- [17] Louis Guttman. “Enlargement Methods for Computing the Inverse Matrix”. In: *The Annals of Mathematical Statistics* 17.3 (1946), pp. 336–343. DOI: 10.1214/aoms/1177730946. URL: <https://doi.org/10.1214/aoms/1177730946>.
- [18] Martin Heusel et al. *GANs Trained by a Two Time-Scale Update Rule Converge to a Local Nash Equilibrium*. 2018. arXiv: 1706.08500 [cs.LG].
- [19] Matt Hoffman et al. “Stochastic Variational Inference”. In: *Screen* 38.3 (June 2012), pp. 282–286. ISSN: 00369543. arXiv: 1206.7051. URL: <http://arxiv.org/abs/1206.7051>.
- [20] M.F. Hutchinson. “A stochastic estimator of the trace of the influence matrix for laplacian smoothing splines”. In: *Communications in Statistics - Simulation and Computation* 19.2 (1990), pp. 433–450. DOI: 10.1080/03610919008812866. eprint: <https://doi.org/10.1080/03610919008812866>. URL: <https://doi.org/10.1080/03610919008812866>.
- [21] Sergey Ioffe and Christian Szegedy. *Batch Normalization: Accelerating Deep Network Training by Reducing Internal Covariate Shift*. 2015. arXiv: 1502.03167 [cs.LG].
- [22] Tommi S. Jaakkola and Michael I. Jordan. “Computing Upper and Lower Bounds on Likelihoods in Intractable Networks”. In: *Proceedings of the Twelfth international conference on Uncertainty in artificial intelligence* 1 (1996), pp. 340–348. URL: <http://dl.acm.org/citation.cfm?id=2074284>. 2074324%7B%5C%7D5Cnhttp://citeseerx.ist.psu.edu/viewdoc/summary?doi=10.1.1.48.5598.
- [23] Michael Karow, Diederich Hinrichsen, and Anthony J Pritchard. “Interconnected systems with uncertain couplings: Explicit formulae for mu-values, spectral value sets, and stability radii”. In: *SIAM journal on control and optimization* 45.3 (2006), pp. 856–884.
- [24] Diederik P Kingma and Max Welling. “Auto-Encoding Variational Bayes”. In: *MI* (2013), pp. 1–14. ISSN: 1312.6114v10. DOI: 10.1051/0004-6361/201527329. arXiv: 1312.6114. URL: <http://arxiv.org/abs/1312.6114>.
- [25] Diederik P Kingma and Max Welling. *Auto-Encoding Variational Bayes*. 2014. arXiv: 1312.6114 [stat.ML].
- [26] Diederik P. Kingma and Jimmy Ba. *Adam: A Method for Stochastic Optimization*. 2017. arXiv: 1412.6980 [cs.LG].
- [27] Durk P Kingma and Prafulla Dhariwal. “Glow: Generative Flow with Invertible 1x1 Convolutions”. In: *Advances in Neural Information Processing Systems*. Ed. by S. Bengio et al. Vol. 31. Curran Associates, Inc., 2018. URL: <https://proceedings.neurips.cc/paper/2018/file/d139db6a236200b21cc7f752979132d0-Paper.pdf>.
- [28] Jack Klys, Jake Snell, and Richard Zemel. “Learning Latent Subspaces in Variational Autoencoders”. In: *32nd Conference on Neural Information Processing Systems (NIPS 2018), Montréal, Canada*. 2018.
- [29] D.A. Knoll and D.E. Keyes. “Jacobian-free Newton–Krylov methods: a survey of approaches and applications”. In: *Journal of Computational Physics* 193.2 (Jan. 2004), pp. 357–397. DOI: 10.1016/j.jcp.2003.08.010. URL: <https://doi.org/10.1016/j.jcp.2003.08.010>.
- [30] David A. Knowles and Thomas P. Minka. “Non-conjugate Variational Message Passing for multinomial and binary regression”. In: *Advances in Neural Information Processing Systems 24: 25th Annual Conference on Neural Information Processing Systems 2011, NIPS 2011* (2011), pp. 1–9.
- [31] Alex Krizhevsky. “Learning Multiple Layers of Features from Tiny Images”. In: (2009), pp. 32–33. URL: <https://www.cs.toronto.edu/~kriz/learning-features-2009-TR.pdf>.
- [32] Yann LeCun and Corinna Cortes. “MNIST handwritten digit database”. In: (2010). URL: <http://yann.lecun.com/exdb/mnist/>.
- [33] Steven Cheng-Xian Li, Bo Jiang, and Benjamin Marlin. “Learning from Incomplete Data with Generative Adversarial Networks”. In: *International Conference on Learning Representations*. 2019. URL: <https://openreview.net/forum?id=S11DV3RcKm>.
- [34] Winfried Lohmiller and Jean-Jacques E Slotine. “On contraction analysis for non-linear systems”. In: *Automatica* 34.6 (1998), pp. 683–696.
- [35] Cheng Lu et al. “Implicit Normalizing Flows”. In: *International Conference on Learning Representations*. 2021. URL: <https://openreview.net/forum?id=8PS8m9oYtNy>.
- [36] Emile Mathieu and Maximilian Nickel. “Riemannian Continuous Normalizing Flows”. In: (2020), arXiv: 2006.10605. URL: <http://arxiv.org/abs/2006.10605>.

- [37] Riccardo Moriconi, Marc P. Deisenroth, and K. S. Sesh Kumar. *High-dimensional Bayesian optimization using low-dimensional feature spaces*. 2020. arXiv: 1902.10675 [stat.ML].
- [38] Vinod Nair and Geoffrey E. Hinton. “Rectified Linear Units Improve Restricted Boltzmann Machines”. In: *Proceedings of the 27th International Conference on International Conference on Machine Learning*. ICML’10. Haifa, Israel: Omnipress, 2010, pp. 807–814. ISBN: 9781605589077.
- [39] Ronald C. Neath. “On Convergence Properties of the Monte Carlo EM Algorithm”. In: *Advances in Modern Statistical Theory and Applications: A Festschrift in honor of Morris L. Eaton*. Institute of Mathematical Statistics, 2013, pp. 43–62. DOI: 10.1214/12-imscol11003. URL: <https://doi.org/10.1214/12-imscol11003>.
- [40] Tan M. Nguyen et al. *InfoCNF: An Efficient Conditional Continuous Normalizing Flow with Adaptive Solvers*. 2019. arXiv: 1912.03978 [cs.LG].
- [41] Derek Onken et al. “OT-Flow: Fast and Accurate Continuous Normalizing Flows via Optimal Transport”. In: (May 2020). arXiv: 2006.00104. URL: <http://arxiv.org/abs/2006.00104>.
- [42] K. B. Petersen and M. S. Pedersen. *The Matrix Cookbook*. Version 20081110. Oct. 2008. URL: <http://www2.imm.dtu.dk/pubdb/p.php?3274>.
- [43] Danilo Jimenez Rezende and Shakir Mohamed. “Variational inference with normalizing flows”. In: *32nd International Conference on Machine Learning, ICML 2015*. Vol. 2. 2015, pp. 1530–1538. ISBN: 9781510810587. arXiv: 1505.05770.
- [44] Trevor W. Richardson et al. *MCFLOW: Monte Carlo Flow Models for Data Imputation*. 2020. arXiv: 2003.12628 [cs.LG].
- [45] Youcef Saad and Martin H. Schultz. “GMRES: A Generalized Minimal Residual Algorithm for Solving Nonsymmetric Linear Systems”. In: *SIAM Journal on Scientific and Statistical Computing* 7.3 (July 1986), pp. 856–869. ISSN: 0196-5204. DOI: 10.1137/0907058. URL: <http://dx.doi.org/10.1137/0907058>.
- [46] Valeria Simoncini and Daniel B. Szyld. “Recent computational developments in Krylov subspace methods for linear systems”. In: *Numerical Linear Algebra with Applications* 14.1 (2007), pp. 1–59. ISSN: 10705325. DOI: 10.1002/nla.499.
- [47] Eduardo D Sontag. *Mathematical control theory: deterministic finite dimensional systems*. Vol. 6. Springer Science & Business Media, 2013.
- [48] Jakub M. Tomczak and Max Welling. “Improving Variational Auto-Encoders using Householder Flow”. In: 2 (2016). arXiv: 1611.09630. URL: <http://arxiv.org/abs/1611.09630>.
- [49] Duc N Tran, Björn S Rüffer, and Christopher M Kellett. “Incremental stability properties for discrete-time systems”. In: *2016 IEEE 55th Conference on Decision and Control (CDC)*. IEEE, 2016, pp. 477–482.
- [50] Brian L Trippe and Richard E Turner. *Conditional Density Estimation with Bayesian Normalizing Flows*. 2018. arXiv: 1802.04908 [stat.ML].
- [51] Martin J Wainwright and Michael I Jordan. “Graphical models, exponential families, and variational inference”. In: *Foundations and Trends in Machine Learning* 1.1-2 (2008), pp. 1–305. ISSN: 19358237. DOI: 10.1561/22000000001.
- [52] Yaqing Wang et al. *Generalizing from a Few Examples: A Survey on Few-Shot Learning*. 2020. arXiv: 1904.05046 [cs.LG].
- [53] Christina Winkler et al. *Learning Likelihoods with Conditional Normalizing Flows*. 2019. arXiv: 1912.00042 [cs.LG].
- [54] Jinsung Yoon, James Jordon, and Mihaela van der Schaar. “GAIN: Missing Data Imputation using Generative Adversarial Nets”. In: *Proceedings of the 35th International Conference on Machine Learning*. Ed. by Jennifer Dy and Andreas Krause. Vol. 80. Proceedings of Machine Learning Research. PMLR, Oct. 2018, pp. 5689–5698. URL: <http://proceedings.mlr.press/v80/yoon18a.html>.

## Checklist

The checklist follows the references. Please read the checklist guidelines carefully for information on how to answer these questions. For each question, change the default **[TODO]** to **[Yes]**, **[No]**, or **[N/A]**. You are strongly encouraged to include a **justification to your answer**, either by referencing the appropriate section of your paper or providing a brief inline description. For example:

- Did you include the license to the code and datasets? **[Yes]** See Section ??.
- Did you include the license to the code and datasets? **[No]** The code and the data are proprietary.
- Did you include the license to the code and datasets? **[N/A]**

Please do not modify the questions and only use the provided macros for your answers. Note that the Checklist section does not count towards the page limit. In your paper, please delete this instructions block and only keep the Checklist section heading above along with the questions/answers below.

1. For all authors...
  - (a) Do the main claims made in the abstract and introduction accurately reflect the paper's contributions and scope? **[Yes]**
  - (b) Did you describe the limitations of your work? **[Yes]**
  - (c) Did you discuss any potential negative societal impacts of your work? **[No]** We do not see what negative social impact this work could have.
  - (d) Have you read the ethics review guidelines and ensured that your paper conforms to them? **[Yes]**
2. If you are including theoretical results...
  - (a) Did you state the full set of assumptions of all theoretical results? **[Yes]**
  - (b) Did you include complete proofs of all theoretical results? **[Yes]**
3. If you ran experiments...
  - (a) Did you include the code, data, and instructions needed to reproduce the main experimental results (either in the supplemental material or as a URL)? **[No]** The data is public, but the code is proprietary. Sadly, we did not get the permission to share it.
  - (b) Did you specify all the training details (e.g., data splits, hyperparameters, how they were chosen)? **[Yes]**
  - (c) Did you report error bars (e.g., with respect to the random seed after running experiments multiple times)? **[No]** When possible, we provided the 95% CI. We compare against benchmarks that did not report the error bars. Experiments were not run across multiple seeds but across multiple items.
  - (d) Did you include the total amount of compute and the type of resources used (e.g., type of GPUs, internal cluster, or cloud provider)? **[Yes]**
4. If you are using existing assets (e.g., code, data, models) or curating/releasing new assets...
  - (a) If your work uses existing assets, did you cite the creators? **[Yes]**
  - (b) Did you mention the license of the assets? **[No]**
  - (c) Did you include any new assets either in the supplemental material or as a URL? **[No]**
  - (d) Did you discuss whether and how consent was obtained from people whose data you're using/curating? **[Yes]** The data we used are publicly available.
  - (e) Did you discuss whether the data you are using/curating contains personally identifiable information or offensive content? **[No]** The data we use is quite common (MNIST and CIFAR) and does not contains identifiable information.
5. If you used crowdsourcing or conducted research with human subjects...
  - (a) Did you include the full text of instructions given to participants and screenshots, if applicable? **[N/A]**
  - (b) Did you describe any potential participant risks, with links to Institutional Review Board (IRB) approvals, if applicable? **[N/A]**
  - (c) Did you include the estimated hourly wage paid to participants and the total amount spent on participant compensation? **[N/A]**

## A Existence of the complementary restriction $g^H$

There are many ways to prove the existence of the complementary restriction  $g^H$ . We rely on Guttman rank additivity formula [16]: if  $\mathbf{J}^{OO} = \nabla_{\mathbf{x}^O} f^O(\mathbf{x}^O; \mathbf{x}^H)$  is a submatrix of a full-rank matrix  $\mathbf{J}$  and is itself full-rank, then

$$\text{rank}(\mathbf{J}) = \text{rank}(\mathbf{J}^{OO}) - \text{rank}\left(\mathbf{J}^{HH} + \mathbf{J}^{HO} (\mathbf{J}^{OO})^{-1} \mathbf{J}^{OH}\right).$$

It is easy to see that in this case, the block  $\mathbf{J}^{HH} - \mathbf{J}^{HO} (\mathbf{J}^{OO})^{-1} \mathbf{J}^{OH}$  is also full-rank, and its inverse is given by  $\mathbf{G}^{HH}$  which is the Jacobian matrix  $\nabla_{\mathbf{y}^H} g^H(\mathbf{y}^H; \mathbf{y}^O)$ . Notice that a similar proof could be derived using the Schur determinant identity. Also, interestingly, the original result by Guttman already showed that if  $\mathbf{J}$  and  $\mathbf{J}^{OO}$  are invertible then so is  $\mathbf{J}^{HH} - \mathbf{J}^{HO} (\mathbf{J}^{OO})^{-1} \mathbf{J}^{OH}$  (see Section 4 in [17]).

Assumption 1 also states that the absolute value of the eigenvalues of  $\mathbf{J}^{OO}$  must be greater than some small  $\varepsilon$  with  $\varepsilon > 0$ . This technical assumption is required to make sure that the eigenvalues of  $\mathbf{G}^{HH}$  are also bounded. Otherwise, the two parts of the decomposition of the LAD Jacobian in Eq 2 may become extremely distant (far greater and lower than 0) and numerically hard to work with.

## B Theorem 1: A convergence result

For convenience we restate the theorem.

**Theorem 1** Consider Algorithm 2, assume that there exists a unique solution  $\widetilde{\mathbf{x}}^O = g^O(\mathbf{y}^O, \widetilde{\mathbf{y}}^H)$ ,  $\widetilde{\mathbf{y}}^H = f^H(\widetilde{\mathbf{x}}^O, \mathbf{x}^H)$  around which  $g^O$  and  $f^H$  are continuously-differentiable, and the global Lipschitz constants of  $f^H$  and  $g^O$  are equal to  $L_a$  and  $L_b$ , respectively. Then the algorithm converges to the unique solution for any  $\alpha \in (0, 1]$ ,  $\beta \in (0, 1]$ , if  $L_a L_b < 1$ .

We argue convergence of the iterative procedure using dynamical systems theory and the notion of stability (cf., [47]). In general, stability is a stronger property than convergence, as stability requires convergence under perturbations in the initial conditions of an iterative procedure. We will prove the theorem in Proposition 1, in what follows, but first we need to develop theoretical notions of stability.

Recall that the updates in the algorithm are as follows:

$$\begin{aligned}\widetilde{\mathbf{y}}^H &:= \alpha f^H(\widetilde{\mathbf{x}}^O, \mathbf{x}^H) + (1 - \alpha) \widetilde{\mathbf{y}}^H \\ \widetilde{\mathbf{x}}^O &:= \beta g^O(\mathbf{y}^O, \widetilde{\mathbf{y}}^H) + (1 - \beta) \widetilde{\mathbf{x}}^O\end{aligned}$$

By letting  $\boldsymbol{\eta}$ ,  $\boldsymbol{\xi}$  stand for  $\widetilde{\mathbf{y}}^H$ ,  $\widetilde{\mathbf{x}}^O$ , respectively, and  $a(\cdot) = f^H(\cdot, \mathbf{x}^H)$  and  $b(\cdot) = g^O(\mathbf{y}^O, \cdot)$ , our iterative procedure can be written without loss of generality as the following dynamical system:

$$\begin{aligned}\boldsymbol{\eta}^{k+1} &= (1 - \alpha) \boldsymbol{\eta}^k + \alpha a(\boldsymbol{\xi}^k), \\ \boldsymbol{\xi}^{k+1} &= (1 - \beta) \boldsymbol{\xi}^k + \beta b(\boldsymbol{\eta}^{k+1}).\end{aligned}\tag{8}$$

We now will review stability results, which are presented for the systems  $\boldsymbol{\zeta}^{k+1} = \mathbf{C}(\boldsymbol{\zeta}^k)$  with the initial state  $\boldsymbol{\zeta}^0 = \boldsymbol{\nu}$ , we will denote systems' trajectories as  $\boldsymbol{\zeta}^k(\boldsymbol{\nu})$ . In our bounds, we will make use of the class of  $\mathcal{KL}$  functions. The function  $\gamma \in \mathcal{KL}$  if  $\gamma : \mathbb{R}_{\geq 0} \times \mathbb{R}_{\geq 0} \rightarrow \mathbb{R}_{\geq 0}$ ,  $\gamma$  is continuous and strictly increasing in the first argument, continuous and strictly decreasing in the second argument, with  $\lim_{t \rightarrow \infty} \gamma(\zeta, k) = 0$  for every  $\zeta$ ,  $\gamma(0, k) = 0$  for all  $k \geq 0$ .

**Definition 1** A system is called globally asymptotically stable at  $\boldsymbol{\zeta}^*$  if there exists a function  $\gamma \in \mathcal{KL}$  such that for all  $\boldsymbol{\nu}$  and all  $k$ :

$$\|\boldsymbol{\zeta}^k(\boldsymbol{\nu}) - \boldsymbol{\zeta}^*\| \leq \gamma(\|\boldsymbol{\nu} - \boldsymbol{\zeta}^*\|, k),$$

Stability theory offers many additional tools, for instance, the ability of studying how trajectories behave in comparison to each other, which can be done using contraction theory [34] or using a similar concept of incremental stability[49].

**Definition 2** A system is called globally asymptotically incrementally stable if there exists a function  $\gamma$  such that for all  $\boldsymbol{\nu}_1, \boldsymbol{\nu}_2$  and all  $k$ :

$$\|\zeta^k(\boldsymbol{\nu}_2) - \zeta^k(\boldsymbol{\nu}_1)\| \leq \gamma(\|\boldsymbol{\nu}_2 - \boldsymbol{\nu}_1\|, k),$$

In our derivation, we will also employ local convergence concepts and results

**Definition 3** A system is called locally asymptotically stable at  $\zeta^*$  if there exist a function  $\gamma$  and  $\varepsilon > 0$  such that for all  $\|\boldsymbol{\nu} - \zeta^*\| < \varepsilon$  and all  $k$ :

$$\|\zeta^k(\boldsymbol{\nu}) - \zeta^*\| \leq \gamma(\|\boldsymbol{\nu} - \zeta^*\|, k),$$

Checking local stability is rather straightforward given some regularity conditions. In particular, we need to check the magnitude of the spectral radius of  $\partial C(\zeta)$ . Recall that spectral radius  $\rho(\mathbf{D})$  is defined as  $\rho = \max_i |\lambda_i(\mathbf{D})|$ , where  $\lambda_i$  are the eigenvalues of  $\mathbf{D}$ .

**Lemma 2** Let  $\mathbf{A}$  be continuously-differentiable around  $\zeta^*$ . If the spectral radius  $\rho(\partial C(\zeta^*))$  is strictly smaller than one, then the system is locally asymptotically stable around  $\zeta^*$ . If  $C(\zeta)$  is a linear function, then the system is also globally stable.

We also have this lemma linking incremental stability and stability properties, which can be shown in a straightforward manner.

**Lemma 3** If the system  $\zeta^{k+1} = C(\zeta^k)$  is locally asymptotically stable around  $\zeta^*$  and globally asymptotically incrementally stable, then it is also globally asymptotically stable.

Finally, we need the following lemma, which is a combination of two results discussed in [23]: properties of nonnegative matrices (the property  $\rho_2$ ) and Lemma 4.1., which follows the introduction of these properties.

**Lemma 4** Let  $\mathbf{C}_{jk} \in \mathbb{R}^{l_j \times l_k}$ ,  $\|\cdot\|$  is the singular value matrix norm, and  $\|\mathbf{C}_{jk}\| \leq c_{jk}$  then

$$\rho \left( \begin{pmatrix} \mathbf{C}_{11} & \dots & \mathbf{C}_{1m} \\ \vdots & & \vdots \\ \mathbf{C}_{m1} & \dots & \mathbf{C}_{mm} \end{pmatrix} \right) \leq \rho \left( \begin{pmatrix} \|\mathbf{C}_{11}\| & \dots & \|\mathbf{C}_{1m}\| \\ \vdots & & \vdots \\ \|\mathbf{C}_{m1}\| & \dots & \|\mathbf{C}_{mm}\| \end{pmatrix} \right) \leq \rho \left( \begin{pmatrix} c_{11} & \dots & c_{1m} \\ \vdots & & \vdots \\ c_{m1} & \dots & c_{mm} \end{pmatrix} \right).$$

Now we are ready to proceed with the proof.

**Proposition 1** The system (8) is globally asymptotically incrementally stable for any  $\alpha, \beta \in (0, 1)$  if  $L_a L_b < 1$ . Furthermore, if there exists  $\xi^*, \eta^*$  such that  $\xi^* = a(\eta^*)$ ,  $\eta^* = b(\xi^*)$ , then the system is globally asymptotically stable.

**Proof:** First let us show incremental stability. Let  $\delta\eta^k = \eta_1^k - \eta_2^k$ ,  $\delta\eta^{k+1} = \eta_1^{k+1} - \eta_2^{k+1}$ ,  $\delta\xi^k = \xi_1^k - \xi_2^k$ , and  $\delta\xi^{k+1} = \xi_1^{k+1} - \xi_2^{k+1}$ , then we have

$$\begin{aligned} \|\delta\eta^{k+1}\| &= \|\eta_1^{k+1} - \eta_2^{k+1}\| = \|(1 - \alpha)(\eta_1^k - \eta_2^k) + \alpha(a(\xi_1^k) - a(\xi_2^k))\| \leq \\ &(1 - \alpha)\|\eta_1^k - \eta_2^k\| + \alpha\|a(\xi_1^k) - a(\xi_2^k)\| \leq (1 - \alpha)\|\delta\eta^k\| + \alpha L_a \|\delta\xi^k\|. \end{aligned}$$

Similarly

$$\begin{aligned} \|\delta\xi^{k+1}\| &= \|\xi_1^{k+1} - \xi_2^{k+1}\| = \|(1 - \beta)(\xi_1^k - \xi_2^k) + \beta(b(\eta_1^{k+1}) - b(\eta_2^{k+1}))\| \leq \\ &(1 - \beta)\|\xi_1^k - \xi_2^k\| + \beta\|b(\eta_1^{k+1}) - b(\eta_2^{k+1})\| \leq (1 - \beta)\|\delta\xi^k\| + \beta L_b \|\delta\eta^{k+1}\| \leq \\ &((1 - \beta) + \alpha\beta L_a L_b)\|\delta\xi^k\| + (1 - \alpha)\beta L_b \|\delta\eta^k\|. \end{aligned}$$

Summarising we have the following bounds

$$\begin{aligned} \|\delta\eta^{k+1}\| &\leq (1 - \alpha)\|\delta\eta^k\| + \alpha L_a \|\delta\xi^k\|, \\ \|\delta\xi^{k+1}\| &\leq (1 - \alpha)\beta L_b \|\delta\eta^k\| + ((1 - \beta) + \alpha\beta L_b L_a)\|\delta\xi^k\|, \end{aligned} \tag{9}$$

which we can equivalently write in the matrix form:

$$\begin{pmatrix} \|\delta\boldsymbol{\eta}^{k+1}\| \\ \|\delta\boldsymbol{\xi}^{k+1}\| \end{pmatrix} \leq \begin{pmatrix} 1 - \alpha & \alpha L_a \\ (1 - \alpha)\beta L_b & (1 - \beta) + \alpha\beta L_b L_a \end{pmatrix} \begin{pmatrix} \|\delta\boldsymbol{\eta}^k\| \\ \|\delta\boldsymbol{\xi}^k\| \end{pmatrix}. \quad (10)$$

As these bounds are valid for every step  $k$ , we can study convergence of  $\|\delta\boldsymbol{\eta}^k\|$ ,  $\|\delta\boldsymbol{\xi}^k\|$  using the system:

$$\begin{pmatrix} z_1^{k+1} \\ z_2^{k+1} \end{pmatrix} = \underbrace{\begin{pmatrix} 1 - \alpha & \alpha L_a \\ (1 - \alpha)\beta L_b & 1 - \beta + \alpha\beta L_b L_a \end{pmatrix}}_{\mathbf{C}} \begin{pmatrix} z_1^k \\ z_2^k \end{pmatrix}.$$

Indeed, if  $|z_1^k|^2 + |z_2^k|^2$  converges to zero as  $k \rightarrow \infty$ , then  $\|\delta\boldsymbol{\eta}^k\|^2 + \|\delta\boldsymbol{\xi}^k\|^2$  also converges to zero as  $k \rightarrow \infty$ . According to Lemma 2 as long as the matrix  $\mathbf{C}$  has the largest absolute value of the eigenvalues smaller than one, the sequence  $\{|z_1^k|^2 + |z_2^k|^2\}$  converges to zero as  $k \rightarrow \infty$  for any initialization  $z_1^0 = \|\delta\boldsymbol{\eta}^0\|$ ,  $z_2^0 = \|\delta\boldsymbol{\xi}^0\|$ . This would imply that  $\|\delta\boldsymbol{\eta}^k\|^2 + \|\delta\boldsymbol{\xi}^k\|^2$  converges to zero as  $k \rightarrow \infty$  and hence the system (8) is global asymptotic incremental stability.

Now all we need to show is that the spectral radius is strictly smaller than one. First, we make a simple transformation obtained by a change of variables  $z_2 = \sqrt{\frac{(1-\alpha)\beta L_b}{\alpha L_a}} \tilde{z}_2$  resulting in the following dynamical system

$$\begin{pmatrix} z_1^{k+1} \\ \tilde{z}_2^{k+1} \end{pmatrix} = \underbrace{\begin{pmatrix} 1 - \alpha & \sqrt{\alpha(1 - \alpha)\beta L_a L_b} \\ \sqrt{\alpha(1 - \alpha)\beta L_a L_b} & 1 - \beta + \alpha\beta L_b L_a \end{pmatrix}}_{\tilde{\mathbf{C}}} \begin{pmatrix} z_1^k \\ \tilde{z}_2^k \end{pmatrix}.$$

Since the system matrix  $\tilde{\mathbf{C}}$  is symmetric, all we have to do is derive the conditions when

$$\begin{pmatrix} 1 - \alpha & \sqrt{\alpha(1 - \alpha)\beta L_a L_b} \\ \sqrt{\alpha(1 - \alpha)\beta L_a L_b} & 1 - \beta + \alpha\beta L_b L_a \end{pmatrix} \prec \begin{pmatrix} 1 & 0 \\ 0 & 1 \end{pmatrix},$$

which is equivalent to

$$\begin{pmatrix} \alpha & \sqrt{\alpha(1 - \alpha)\beta L_a L_b} \\ \sqrt{\alpha(1 - \alpha)\beta L_a L_b} & \beta - \alpha\beta L_a L_b \end{pmatrix} \succ 0 \iff \\ \alpha\beta - \alpha^2\beta L_a L_b > \alpha(1 - \alpha)\beta L_a L_b \iff \alpha\beta > \alpha\beta L_a L_b \iff 1 > L_a L_b.$$

This proves that  $\{|z_1^k|^2 + |\tilde{z}_2^k|^2\}$  and consequently  $\|\delta\boldsymbol{\eta}^k\|^2 + \|\delta\boldsymbol{\xi}^k\|^2$  converge to zero as  $k \rightarrow \infty$ .

Now we need to show that the system is locally asymptotically stable around any solution to  $\boldsymbol{\xi}^* = a(\boldsymbol{\eta}^*)$ ,  $\boldsymbol{\eta}^* = b(\boldsymbol{\xi}^*)$ . Let us compute the Jacobian of the dynamical system (8). Denoting  $\mathbf{A} = \partial a(\boldsymbol{\eta}^*)$   $\mathbf{B} = \partial b(\boldsymbol{\xi}^*)$  we have the following Jacobian

$$\mathbf{C} = \begin{pmatrix} 1 - \alpha & \alpha\mathbf{A} \\ (1 - \alpha)\beta\mathbf{B} & (1 - \beta) + \alpha\beta\mathbf{B}\mathbf{A} \end{pmatrix}$$

Due to the Lipschitz constraint on the function  $a$  and  $b$ , we have  $\|\mathbf{A}\| \leq L_a$  and  $\|\mathbf{B}\| \leq L_b$ . According to Lemma 4, this leads to:

$$\rho(\mathbf{C}) \leq \rho\left(\begin{pmatrix} 1 - \alpha & \alpha\|\mathbf{A}\| \\ \|(1 - \alpha)\beta\mathbf{B}\| & \|(1 - \beta) + \alpha\beta\mathbf{B}\mathbf{A}\| \end{pmatrix}\right) \leq \rho\left(\begin{pmatrix} 1 - \alpha & \alpha L_a \\ (1 - \alpha)\beta L_b & (1 - \beta) + \alpha\beta L_b L_a \end{pmatrix}\right),$$

and finally to  $\rho(\mathbf{C}) < 1$ , local asymptotic stability around the fixed point, as well as global asymptotic stability according to Lemmas 2 and 3.  $\square$

## C On the form of the variational posterior

**Post-training conditional inference** A broad range of variational algorithms impose a fully factorisable form for the approximate posterior, which is usually referred to as the mean-field assumption [19, 5, 24, 22, 51, 30]. In this context, one would usually opt in favour of a diagonal Gaussian distribution



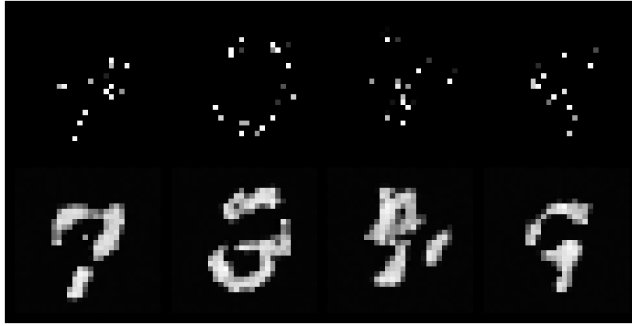


Figure 3: Implicit Normalizing Flow data completion results. Incomplete and completed digits are shown on the first and second row, respectively.

for  $q_\theta$  base distribution. To relax this assumption and bring flexibility to the variational posterior, we relied on Householder flows [48] as a sparse approximation to a full covariance matrix:

$$\mathbf{x} = \boldsymbol{\mu} + \prod_{i=1}^n \mathbf{H}_i D(\boldsymbol{\sigma}) \boldsymbol{\epsilon} \quad (11)$$

where the function  $D$  maps the vector  $\boldsymbol{\sigma}$  to a diagonal matrix. Householder flows consist of a series of  $n$  orthogonal transformation  $\mathbf{H}_i$  of a base vector  $\boldsymbol{\epsilon} \sim \mathcal{N}(0, \mathbf{I})$ . In principle, such maps can model any orthogonal matrix when  $n$  is sufficiently large. The main advantage of this approximate posterior formulation is its time and memory computational cost, as it only requires inner vector-vector and vector-scalar products.

**Learning from incomplete data** A common usage in VAEs is to amortise the construction of parametric variational posteriors by building a so-called inference network that maps each datapoint to its correspondent parameter configuration. In the case of incomplete data, one usually has to deal with missing values that are randomly spread in the data space and whose dimensionality can be hard to foreseen. Inputting such sparse data in a neural network can be challenging. To solve this, we filled every missing value with the median value of the data tensor, thereby creating a workable input for the inference network. In turn, this inference network produced a fully-factorised variational posterior which was indexed according to the latent space partition.

## D MNIST data completion with Implicit Normalizing Flows

We tested the IVCNF algorithm on a data completion task with Implicit Normalizing Flows (INF) [35] to show that our method can be extended beyond iResNet architectures. Unlike iResNet, the Lipschitz constant of a single block of INF is unbounded, making it potentially considerably more expressive. To efficiently train INF, we note that the original problem that is to be solved for one block, which reads

$$F(\mathbf{x}, \mathbf{z}) = \mathbf{x} - \mathbf{z} + f(\mathbf{x}) - g(\mathbf{z}) = 0$$

is equivalent to solving

$$\mathbf{z} = h^{-1}(\mathbf{x} + f(\mathbf{x}))$$

where  $h(\mathbf{z}) = \mathbf{z} + g(\mathbf{z})$  is a iResNet block. We know how to invert  $h$  [3] using fixed-point iterations, and we have already presented how to propagate gradients through this transformation using Neumann series (see Section 4). These two solutions showed to be considerably faster and more memory efficient than the joint use of Brodyen method and linear system solving algorithms presented in the original work.

We trained a convolutional INF network that was defined in a similar manner as the iResNet model designed for the CIFAR task in the main text, with the following notable amendments. First, to match the INF structure, the direction of one every two iResNet blocks was flipped ( $f_i \rightarrow f_i^{-1}$ ) such

that plain and inverted residual blocks alternated. ActNorm layers [27] were interleaved in between iResNet blocks. To compute the higher order gradients required in Eq 7, and since the gradient of inverted iResNet block was computed using Neumann series, we relied once more on the following identity:

$$\nabla_{\mathbf{y}} \mathbf{G}(\mathbf{y}) = \nabla_{\mathbf{y}} (-\mathbf{G} \mathbf{J}(\mathbf{x}(\mathbf{y})) \mathbf{G})$$

where  $\mathbf{G} = \mathbf{J}^{-1} = (\mathbf{I} + \nabla_{\mathbf{x}} f(\mathbf{x}))^{-1}$  is the inverse Jacobian obtained through the truncated series  $\sum_{j=0}^n -(\nabla_{\mathbf{x}} f(\mathbf{x}))^j$ , and the dependence of  $\mathbf{G}$  (or  $\mathbf{x}$ ) on  $\mathbf{y}$  is made explicit where needed. We trained this INF network on the complete MNIST training dataset using the Adam optimiser for 20 epochs with a learning rate of  $10^{-3}$ . We used the IVCNF algorithm to complete digits where 90% of the pixels were missing. The CLADE gradient estimator was used to approximate the gradient of the LAD of the partial Jacobian. Results of this task are displayed in Figure 3. We noticed that the fixed-point algorithm was slightly less effective with INF networks than with iResNet: for a small proportion of the iterations during the optimisation ( $< 30\%$ ), our algorithm did not converge to the solution and required a few Newton-Krylov iterations ( $< 5$ ) to complete the process. It is worth emphasising that, in all cases, the fixed-point algorithm always played a major role in finding the solution of the equality constraint, reducing the distance between the imposed values  $\mathbf{y}^O$ ,  $\mathbf{x}^H$  and their estimate  $f^O(\tilde{\mathbf{x}})$ ,  $g^H(\tilde{\mathbf{y}})$  by more than 90% with respect to the original values. Also, using the same partition of the observed and latent space led us to find a workable solution in every single completion case.